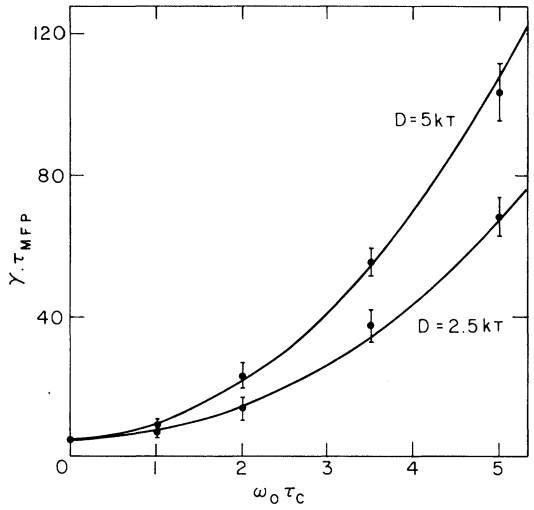

FIG. 1. $\gamma\tau_{MFP}$ vs $\omega_0\tau_c$ for a Morse oscillator from Eq. (23) (lines) and from stochastic classical trajectories (points with error bars). $\gamma/\omega_0 = 0.04$.

Morse oscillator and the model (3) as a function of τ_c. For $D = 2.5kT$ and $5kT$ we compare results calculated from Eqs. (1)–(3) using stochastic classical trajectories to those obtained from Eq. (23). The agreement is good even when J_B corresponds to the dissociation threshold where the low-viscosity condition $\omega \gg \gamma$ does not apply. We also see that τ_c has a profound effect on the rate obtained in the non-Markoffian Kramers model.

This research was supported in part by the U. S.–Israel Binational Science Foundation. We thank E. Ben-Jacob, D. Bergman, M. Bixon, and Z. Schuss for helpful discussions.

[1]H. A. Kramers, Physica (Utrecht) 7, 284 (1940).

[2]Actually the left inequality in (4) may be replaced by the less stringent condition $|Z(\omega)| \ll \tau_c^{-1}$ [$Z(\omega)$ defined by (11)].

[3]M. Shugard, J. C. Tully, and A. Nitzan, J. Chem. Phys. 69, 336, 2525 (1978).

[4]R. W. Zwanzig, Phys. Fluids 2, 12 (1959). R. F. Grote and J. T. Hynes (to be published) have recently applied Zwanzig's approach to arrive at conclusions similar to ours.

[5]R. F. Grote and J. T. Hynes, J. Chem. Phys. 73, 2715 (1980), and 74, 4465 (1981).

[6]M. Lax, Rev. Mod. Phys. 38, 541 (1966).

[7]Unless states otherwise Σ_n denotes a sum from $-\infty$ to ∞.

[8]One can proceed without invoking the rotating-wave approximation, at the cost of more tedious algebra, to arrive at the same final result.

[9]G. H. Weiss, Adv. Chem. Phys. 13, 1 (1966).

Infinite Conical Well: An Analytic Model for Quantum Mechanical Hindered Rotors

J. W. Gadzuk
National Bureau of Standards, Washington, D. C. 20234

and

Uzi Landman, E. J. Kuster, C. L. Cleveland, and R. N. Barnett
Georgia Institute of Technology, School of Physics, Atlanta, Georgia 30332

(Received 17 May 1982)

The rotational quantum mechanics of a new analytic model for a hindered rotor is presented, and rotational-state distributions of the hindered rotor are given in terms of unhindered rotor states.

PACS numbers: 03.65.Ge, 33.10.Ev, 33.70.Ca, 68.45.Da

The role played by the rotational degrees of freedom of diatomic molecules which are dynamically coupled to solid surfaces has been the focus of several recent experiments in which the observed rotational-state distributions of diatomic molecules scattered,[1] desorbed,[2] and sputtered[3] from surfaces bear no obvious relationship to equilibrium state distributions inferred from surface temperatures. In this communication we present the main features and illustrative numer-

ical consequences of a model for a hindered three-dimensional rotor, which provides considerable insight into possible mechanisms responsible for the reported state distributions. The model in which a rigid dumbbell executes free rotations within a conical domain bounded at some critical polar angle $\beta \leq \pi/2$ by an infinitely repulsive wall, and as such is a spherical-coordinate-system analog of a textbook infinite square well, is displayed in the inset of Fig. 1. In Fig. 1(a) the rotations are about an origin placed at the center of mass. This geometry could simulate a hindered rotor embedded within an anisotropic void or in an "atomic trough" on a surface. The rotor shown in Fig. 1(b) simulates an adsorbed diatomic molecule in which one end might be clamped to a surface via a chemical bond. As will become apparent, the model facilitates identification of the special role played by the zero-point kinetic energy associated with the spatial localization of the rotor, both on ground-state properties and on the excitation spectrum. This can be contrasted with the harmonically constrained rotor in which the effects of localization are distributed between kinetic and potential energy.[4,5]

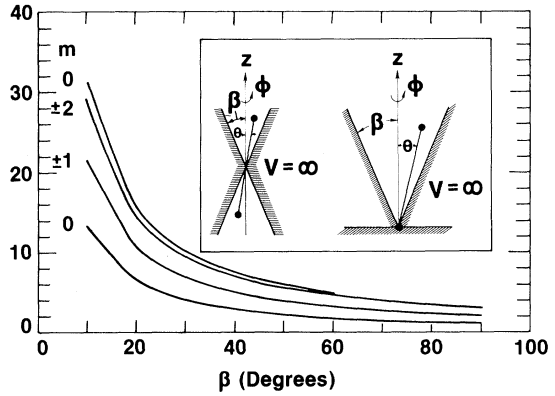

FIG. 1. The four lowest rotational quantum numbers as a function of the cone angle. The azimuthal quantum numbers are labeled on the left. Inset: Infinite conical-well model treated here. The left and right models are referred to as 1(a) and 1(b), respectively.

The model is characterized by the standard angular part of the Schrodinger equation:

$$\left\{\frac{1}{\sin\theta}\frac{\partial}{\partial\theta}\left(\sin\theta\frac{\partial}{\partial\theta}\right)+\frac{1}{\sin^2\theta}\frac{\partial^2}{\partial\varphi^2}+\frac{2I}{\hbar^2}[\epsilon - V(\theta,\varphi)]\right\}\psi^{\mathrm{rot}}(\theta,\varphi)=0, \tag{1}$$

with $I=\sum_i m_i r_i^2$. For the φ-independent "infinite conical well," we have

$$V(\theta,\varphi)=\begin{cases}0, & \theta\leq\beta,\ 0\leq\varphi\leq 2\pi,\\ \infty, & \theta>\beta;\end{cases}$$

so not only is the total rotational wave function separable as

$$\psi^{\mathrm{rot}}(\theta,\varphi)=P(\theta)v(\varphi) \text{ with } v(\varphi)=(2\pi)^{-1/2}\exp(im\varphi)$$

but also $P(\theta)=0$ for $\theta>\beta$. With the above choice for $V(\theta,\varphi)$, it is a textbook exercise to reduce the θ part of Eq. (1), in terms of the auxiliary variable $x=\cos\theta$, to

$$(1-x^2)\frac{d^2P}{dx^2}-2x\frac{dP}{dx}+\left(\frac{2I\epsilon}{\hbar^2}-\frac{m^2}{1-x^2}\right)P=0 \tag{2}$$

valid in the domain $\cos\beta\leq x\leq 1$. Equation (2) is exactly Legendre's equation when the eigenvalues are written in the form

$$\epsilon = B\nu(\nu+1) \tag{3}$$

with $B\equiv\hbar^2/2I$ and ν a continuous (usually noninteger) positive "quantum number." For the free rotor in which $\cos\beta=-1$, the quantum numbers ν take on integer values only and the eigenfunctions ψ_{rot} are the familiar spherical harmonics $Y_{l,m}$. The eigenstates of the hindered rotor, solutions of Eq. (2) with the boundary conditions that $P(x)$ is finite at $x=1$ and zero at $x=\cos\beta$, are associated Legendre functions of arbitrary order,[6] that is

$$\psi_{\nu m}{}^{\mathrm{rot}}(\theta,\varphi)=\begin{cases}A_{\nu m}(2\pi)^{-1/2}P_\nu{}^{|m|}(\cos\theta)\exp(im\varphi), & 0<\theta<\beta,\\ 0, & \beta\leq\theta\leq\pi,\end{cases} \tag{4}$$

with $m^2<\nu(\nu+1)$ and $A_{\nu m}{}^0$ a normalization constant. The eigenvalues are numerically determined by the condition

$$P_\nu{}^m(\cos\beta)=0 \tag{5}$$

together with Eq. (3), and the normalization by

$$|A_{\nu m}|^{-2}=\int_{\cos\beta}^1 dx|P_\nu{}^{|m|}(x)|^2=\frac{-(\nu+m)}{(2\nu+1)}P_{\nu-1}{}^m(\cos\beta)\left[\frac{dP_\nu{}^m(\cos\beta)}{d\nu}\right]. \tag{6}$$

Lastly, the overlap integral between a free space

$$Y_{lm}(\theta,\varphi)=[A_{lm}'/(2\pi)^{1/2}]P_l{}^m(\cos\theta)e^{im\varphi} \quad (l=\text{integer})$$

and $\psi_{\nu m}(\theta,\varphi)$ is easily evaluated with the relationship

$$\langle Y_{lm'}|\psi_{\nu m}\rangle=\frac{\delta_{m,m'}A_{\nu m}A_{lm'}'}{\nu+l+1}\left(\frac{\nu+m}{\nu-l}\right)P_l{}^m(\cos\beta)P_{\nu-1}{}^m(\cos\beta) \tag{7}$$

valid for $\nu\neq l$. Derivations and detailed discussion of the mathematics leading to Eqs. (3)–(7) will be presented in a much expanded article.

An interesting limiting case occurs for $\beta=\pi/2$, that is, when the rotor is constrained to a half-infinite space. The boundary condition, Eq. (5), requires that the eigenfunctions have nodes on the plane separating the two half spaces. But solutions of Eqs. (2) and (4) are just the subset of usual Y_{lm}'s satisfying the "surface-selection rule"[7]

$$l+m=\text{odd}$$

which has as some consequences the following:

(i) The $\beta=\pi/2$ confined-rotor ground state is a nondegenerate p state with $l=\nu=1$, $m=0$.

(ii) The zero-point energy associated with localization of the rotor to a half space is $E_{zp}(\beta=\pi/2)=\hbar^2/I$.

(iii) The lth level is l-fold degenerate rather than $(2l+1)$-fold as in the unhindered rotor.

The lowest four eigenvalues of the hindered rotor, obtained by numerical solution of Eqs. (2), (3), and (5), are displayed in Fig. 1 in the form of ν versus β plots. These results are in accord with our intuition. As β decreases, the zero-point kinetic energy associated with the increased localization increases dramatically, as does the scale of the excitation spectrum. To illustrate the significance of this effect, consider a rotor constrained to a cone with $\beta=10^\circ$, as a model for a diatomic molecule adsorbed in an upright configuration on a surface. With established values for free space rotational constants of N_2 and H_2, the zero-point rotational energies are ~ 0.025 and 1.0 eV, respectively, which in the case of H_2 significantly influences possible chemistry.[5] Moreover, even for N_2 the lowest excitation energy ~ 0.04 eV $\simeq 500$ K, which suggests that most properties of the hindered N_2 will appear temperature independent if the ambient temperature is less than ~ 500 K.

Now consider a model dynamics problem in which the hindering potential in Fig. 1(a) is suddenly switched off[8] (constrained → free rotor transition as might be experienced in thermal desorption), resulting in a nonequilibrium population of free rotational states due to the conversion of initial zero-point kinetic energy into free rotational energy about the rotor center of mass. The probability for ending up in the lth free rotor state is just a sum of rotational Franck-Condon factors between $Y_{lm'}{}^{\text{free}}$ and $\psi_{\nu,m}{}^{\text{rot}}$, given by Eq. (4) weighted by appropriate thermal factors[8]; that is,

$$P(l)=\frac{1}{Z_{\text{hin}}}\sum_{\nu>1,m,m'}\exp[-B\nu(\nu+1)/kT]\,|\langle Y_{lm'}{}^{\text{free}}|\psi_{\nu m}{}^{\text{rot}}\rangle|^2, \tag{8}$$

where T is the ambient temperature and Z_{hin} the hindered-rotor partition function. If $B/kT\gg 1$, one would expect that the population of high-l states results mainly from their overlap with low-lying ν states, not from a one-to-one correspondence with thermally excited ν states. In other words the final-state rotational energy derives from the zero-point energy, not from thermal excitation. Consequently the more narrow the cone, the "hotter" the final-state distribution, independent of ambient temperature. State distributions given by Eq. (8), with values of ν and the overlap integral determined from Eqs. (5)–(7), for a "typical" value of $B/kT=0.05$ (corresponding to say $\theta_r\simeq 15$ K, $T\simeq 300$ K) and treating β parametrically are shown in Fig. 2. As

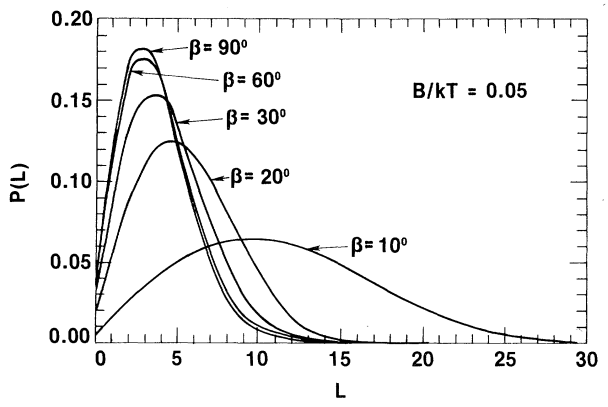

FIG. 2. Rotational-state distributions for the suddenly unhindered rotor of Fig. 1(a), as a function of the free-rotor rotational quantum number.

anticipated, the smaller the hindrance angle, the greater the population of higher-energy rotational states.

Laser-induced-fluorescence data[1-3] are often plotted in the form $\log[P(l)/(2l+1)]$ vs $l(l+1)$, which yields a straight line with slope $=-B/kT_r$ if the rotational distribution of the interogated molecules corresponded to an equilibrium state at some rotational temperature T_r. In fact Kleyn, Luntz, and Auerbach[1] observe two regimes in rotational distributions of NO scattered from Ag. For $l \lesssim 20$, the distribution is Maxwell-Boltzmann, over two orders of magnitude, showing a T_r which is basically independent of the surface temperature. For $l \gtrsim 20$, a plateau structure whose breadth depends upon the kinetic energy of the incident beam is observed. This structure has been attributed to a rotational rainbow.[9] Cavanagh and King[2] also observed a linear distribution over an order of magnitude, for NO thermally desorbed from Ru, again with T_r apparently unrelated to the surface temperature from which the NO desorbed. Efstathiou and Thomas[3] observed distributions similar to those of Kleyn, Luntz, and Auerbach for sputtered N_2 from Si.

Guided purely by the just-mentioned experimental convention for data presentation, we have plotted our state distributions, obtained from Eq. (8), semilogarithmically. The somewhat astonishing results are shown in Fig. 3 where each panel corresponds to a different hindrance angle and B/kT is treated parametrically within a panel. Note that all the distributions show basically two distinctly different regimes. First, for low l ($\lesssim 20$–30), a rather linear decrease occurs over 2 to 3 orders of magnitude whose inverse slope could be represented by a free rotational temperature, as observed.[1-3] As depicted in Fig. 3, for given hindrance angle β, T_r appears to be independent of T (for $\beta \lesssim 45°$). Furthermore, as β decreases the inverse slope or apparent rotational temperature increases. Both of these characteristics support our conjecture that conversion of zero-point rather than thermal kinetic energy into free rotational energy is the mechanism responsible for population of the free-rotor excited states, at least within the context of our model problem; hence the apparent T independence of the low-l state distribution. For model 1(a) treated here (see Fig. 1), T_r is always greater than $2B/k$, the minimum possible zero-point energy (for $\beta=\pi/2$). Thus the distribution appears "hot." In the case of desorption, however, not only is the hindering potential turned off but also

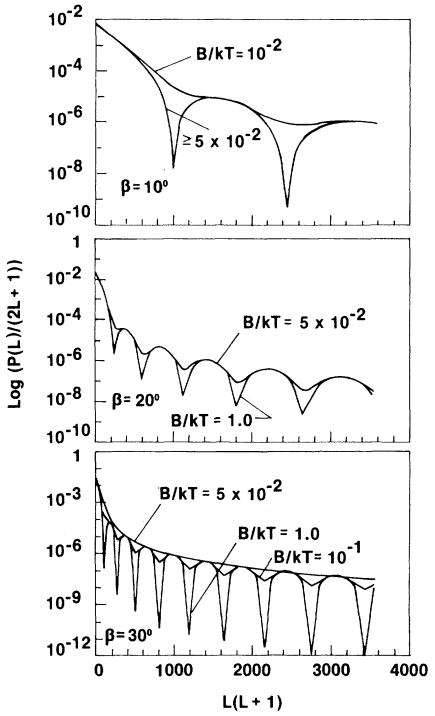

FIG. 3. Rotational-state distributions for the suddenly unhindered rotor of Fig. 1(a), plotted in the form $\log[P(l)/(2l+1)]$ vs $l(l+1)$.

the atom tied down to the surface is released, thus permitting free translation of the molecular center of mass. The addition of this "new" degree of freedom in the final state requires that the rotational zero-point energy is split between translations and free rotations, which would have the effect of cooling our distributions. In fact a simple classical sudden approximation (removal of hindrance and release of tied down atom) on homonuclear model 1(b), with only the consequences of energy and angular momentum conservation, yields the result that $T_r=T/2$, as observed by Cavanagh and King.[2]

The second (high l) region displays qualitatively different behavior. At some critical l value, the state distribution drops precipitously from the linear form, then rises, and displays an oscillatory structure which is most pronounced for large B/kT. The oscillations, which show a periodicity in l varying as $180°/\beta$, are diminished as B/kT decreases, though still leaving a plateau or smoothly varying distribution at high l which is quite different from the low-l range. Already such an effect has been observed in beam[1] and sputtering experiments.[3] The fact that the beam data were interpretable in terms of rotational

rainbows suggests that there could be an intimate connection between the physics responsible for rainbows and the physics implicitly contained within our Franck-Condon factors.

In summary we have presented a model for a hindered diatomic-molecule rotor, worked out its quantum mechanics, and applied the results to a model dynamics problem involving a sudden release of the hindering potential. Conversion of zero-point kinetic energy into free rotational energy results in highly nonequilibrium final rotational-state distributions which have a striking resemblance to state distributions observed in several recent experiments involving different, but related, dynamic surface processes.

This work was supported in part by the U. S. Department of Energy under Contract No. DE-AS05-76ER05489.

[1]A. W. Kleyn, A. C. Luntz, and D. J. Auerbach, Phys. Rev. Lett. 47, 1169 (1981).

[2]R. R. Cavanagh and D. S. King, Phys. Rev. Lett. 47, 1829 (1981).

[3]L. Efstathiou and E. W. Thomas, in Proceedings of the Forty-Second Physical Electronics Conference, 1982 (to be published).

[4]D. White and E. N. Lassettre, J. Chem. Phys. 32, 72 (1960).

[5]I. F. Silvera and M. Nielsen, Phys. Rev. Lett. 37, 1275 (1976); I. F. Silvera, Rev. Mod. Phys. 52, 393 (1980).

[6]*Higher Transcendental Functions*, edited by A. Erdelyi (McGraw-Hill, New York, 1953), Vol. 1.

[7]J. D. Levine, Phys. Rev. 140, A586 (1965); J. W. Gadzuk, Phys. Rev. 154, 662 (1967).

[8]R. B. Bernstein and K. H. Kramer, J. Chem. Phys. 44, 4473 (1964).

[9]R. Schinke, J. Chem. Phys. 76, 2352 (1982), and references therein.

D^{*+} Production in e^+e^- Annihilation at 29 GeV

J. M. Yelton, G. J. Feldman, G. Goldhaber, G. S. Abrams, D. Amidei, A. Bäcker,[a] C. A. Blocker, A. Blondel,[b] A. M. Boyarski, M. Breidenbach, D. L. Burke, W. Chinowsky, G. von Dardel,[c] W. E. Dieterle, J. B. Dillon, J. Dorenbosch,[d] J. M. Dorfan, M. W. Eaton, M. E. B. Franklin, G. Gidal, L. Gladney, L. J. Golding, G. Hanson, R. J. Hollebeek, W. R. Innes, J. A. Jaros, A. D. Johnson, J. A. Kadyk, A. J. Lankford, R. R. Larsen, B. LeClaire, M. Levi, N. Lockyer, B. Löhr,[e] V. Lüth, C. Matteuzzi, M. E. Nelson, J. F. Patrick, M. L. Perl, B. Richter, A. Roussarie,[f] T. Schaad, H. M. Schellman, D. Schlatter, R. F. Schwitters, J. L. Siegrist, J. Strait, G. H. Trilling, R. A. Vidal, Y. Wang,[g] J. M. Weiss, M. Werlen,[h] C. Zaiser, and G. Zhao[g]

Stanford Linear Accelerator Center, Stanford University, Stanford, California 94305, and Lawrence Berkeley Laboratory and Department of Physics, University of California, Berkeley, California 94720, and Department of Physics, Harvard University, Cambridge, Massachusetts 02138

(Received 1 June 1982)

The production of the charmed meson state D^{*+} has been observed in e^+e^- annihilation at 29 GeV. The fragmentation function for charmed quarks appears to be peaked about $z = 0.5$.

PACS numbers: 13.65.+i, 14.40.Jz

In the quark-parton model, quarks produced in high-energy reactions cannot emerge as free entities but materialize as jets of hadronic particles. The quark fragmentation functions describe the dynamical mechanism of the hadronization of quarks into hadrons. The heavy-quark fragmentation functions are of both theoretical and practical interest, but little is known of them. The production of charmed mesons in e^+e^- annihilation provides a clean way for studying the charmed fragmentation function.[1] Previous measurements of the differential cross section $d\sigma/dz$ for inclusive D meson production, where z is the ratio of twice the D energy (E_D) to the center-of-mass energy ($E_{\text{c.m.}}$), were restricted to the kinematic range of $z > 0.54$ available at SPEAR energies.[2,3] Here we present the observation of the D^{*+} by its decay

$$D^{*+} \to D^0\pi^+$$
$$\qquad\quad \hookrightarrow K^-\pi^+$$

